Chem

Diversifying hierarchical ionic assembly by docking cations to anions as salt bridges

Graphical abstract

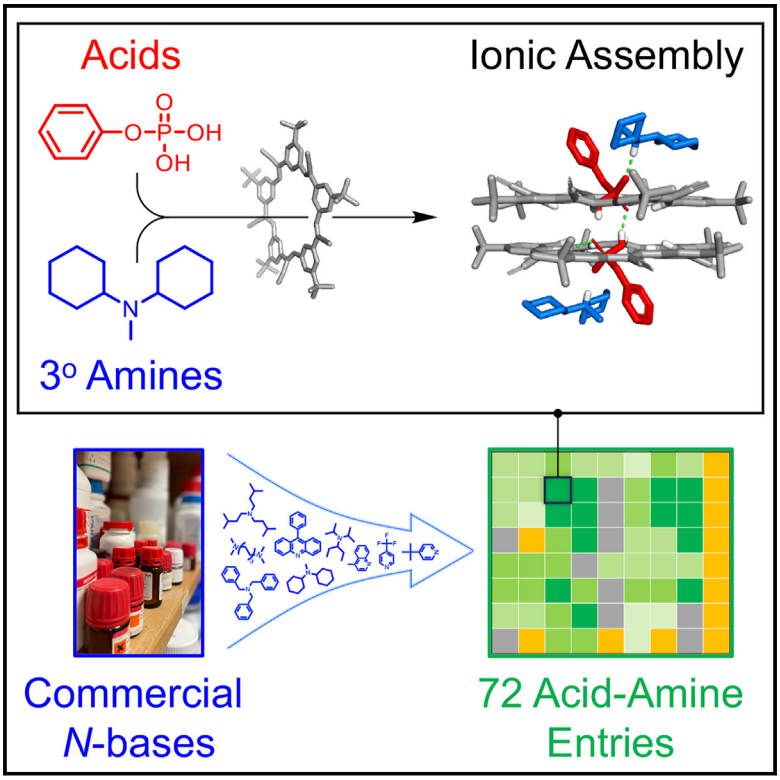

Highlights

- Easy access to ionic building blocks by acid-base chemistry
- Hierarchical assembly of anion dimers inside cyanostars with salt bridges to cations
- High-throughput screen of 72 ion-pair combinations to discover 13 assemblies
- Increased number of cations for assembly by using 3° amines and *N*-heterocyclic bases

Authors

Yusheng Chen, Devika Karolly, Anastasia Kuvayskaya, Maren Pink, Veronica Carta, Alan Sellinger, Amar H. Flood

Correspondence

aflood@iu.edu

In brief

Anion recognition offers new methods for creating self-assembled materials. However, the anions are often paired with inert tetrabutylammonium cations, which limit the diversity of building blocks that can be investigated. We explore simple acid-base chemistry to convert tertiary amines into cations and co-assemble them with phosphates and cyanostar macrocycles into discrete assemblies. Straightforward generation of ionic building blocks allowed high-throughput screening of 72 ion pairs and enabled co-assembly with fluorophores, catalysts, drugs (Cipralex, Zytiga), and ionic liquids.

Chen et al., 2024, Chem *10*, 1–13
December 12, 2024
https://doi.org/10.1016/j.chempr.2024.07.005

CellPress

Please cite this article in press as: Chen et al., Diversifying hierarchical ionic assembly by docking cations to anions as salt bridges, Chem (2024), https://doi.org/10.1016/j.chempr.2024.07.005

Chem

CellPress

Article

Diversifying hierarchical ionic assembly by docking cations to anions as salt bridges

Yusheng Chen,[1] Devika Karolly,[1] Anastasia Kuvayskaya,[2] Maren Pink,[1] Veronica Carta,[4] Alan Sellinger,[2,3] and Amar H. Flood[1,5,*]

[1]Department of Chemistry, Indiana University, 800 E. Kirkwood Avenue, Bloomington, IN 47405, USA
[2]Department of Chemistry, Colorado School of Mines, 1012 14th Street, Golden, CO 80401, USA
[3]National Renewable Energy Laboratory (NREL), 15013 Denver West Parkway, Golden, CO 80401, USA
[4]Department of Chemistry, University of California, Riverside, 501 Big Springs Rd, Riverside, CA 92507, USA
[5]Lead contact
*Correspondence: aflood@iu.edu
https://doi.org/10.1016/j.chempr.2024.07.005

THE BIGGER PICTURE Molecular anions and cations are important organizing elements for creating self-assembled materials. Typically, only one of the two (either anions or cations) is used to direct assembly into an organized structure, leaving the other as a minor spectator. This situation narrows the types of building blocks used for self-assembly and suggests that there might be new opportunities to create diverse supramolecular architectures by involving both anions and cations. We present a simple strategy to activate diverse ammonium cations to co-assemble via salt bridges with various phosphate anions stabilized inside cyanostar macrocycles. Acid-base chemistry is used to generate the ionic building blocks, and with 3,000 amines available commercially, the scope is vast. We screened 19 nitrogen bases, discovered 13 assemblies, and connected them to fluorophores, catalysts, drugs (Cipralex and Zytiga), and ionic liquids. This approach holds promise for producing functional supramolecular materials.

SUMMARY

We expand the diversity of building blocks available for ionic assembly by introducing tertiary (3°) ammonium cations into anion complexes. We use proton transfer between 3° amines and organo-phosphoric acids to generate H-bonding cations (R_3NH^+) and anions ($RHPO_4^-$) that co-assemble with cyanostar macrocycles into assemblies with 2:2:2 stoichiometry. At the heart is a supramolecular dimer where phosphate anions form salt bridges by H-bonding with cations. Unlike conventional 4° ammonium cations, 3,000 commercial amines provide diversity for high-throughput screening of 72 combinations (9 nitrogen bases and 8 acids), producing 13 privileged partners for quantitative assembly. Yields depend on the solvent and sterics of salt bridge formation. Ten more nitrogen bases connect to fluorophores (pyrene), photocatalysts (quinoline), drugs (Cipralex, Zytiga), and ionic liquids (imidazole). The synthesis and examination of 82 new salts exemplify how acid-base chemistry can open a pipeline to a diversity of building blocks for exploring hierarchical ionic assembly.

INTRODUCTION

Cations are emerging as functional and active partners in the hierarchical assembly of anion-driven architectures.[1,2,3,4] Examples include use of cations as templates in phosphate-driven cages,[5,6] fluorescent cations in optical materials,[7,8,9,10] and as structural partners in chemically driven crystallization.[11] At the heart of these assemblies is a receptor-anion complex. They serve as the primary structure upon which higher levels of structural order are layered.[12,13,14,15] Charge-balancing organic and inorganic[3,4,16] cations are a potential source of higher order[17,18,19,20] with crystal structures hinting at what might be possible (Figure 1A). Most studies of anion-driven assembly use quaternary (4°) ammonium as inert cations, and tetra-*n*-butylammonium cation (TBA^+)[21,22,23,24,25,26,27,28,29,30] is typical. The *N*-substitution with four alkyl chains turns off specific interactions,[31] e.g., H-bonds, and structural ordering to help disfavor ion pairing and liberate the anions for binding.[32,33,34] Although this approach has been successful, it comes at the expense of diversity with few exceptions.[3,33] To expand the chemical diversity, we explore use of tertiary (3°) ammonium cations that are easy to make using acid-base chemistry. This strategy also turns on directional H-bonding with the potential for salt bridge formation in the assembly (Figure 1B),[35,36] which is

Please cite this article in press as: Chen et al., Diversifying hierarchical ionic assembly by docking cations to anions as salt bridges, Chem (2024), https://doi.org/10.1016/j.chempr.2024.07.005

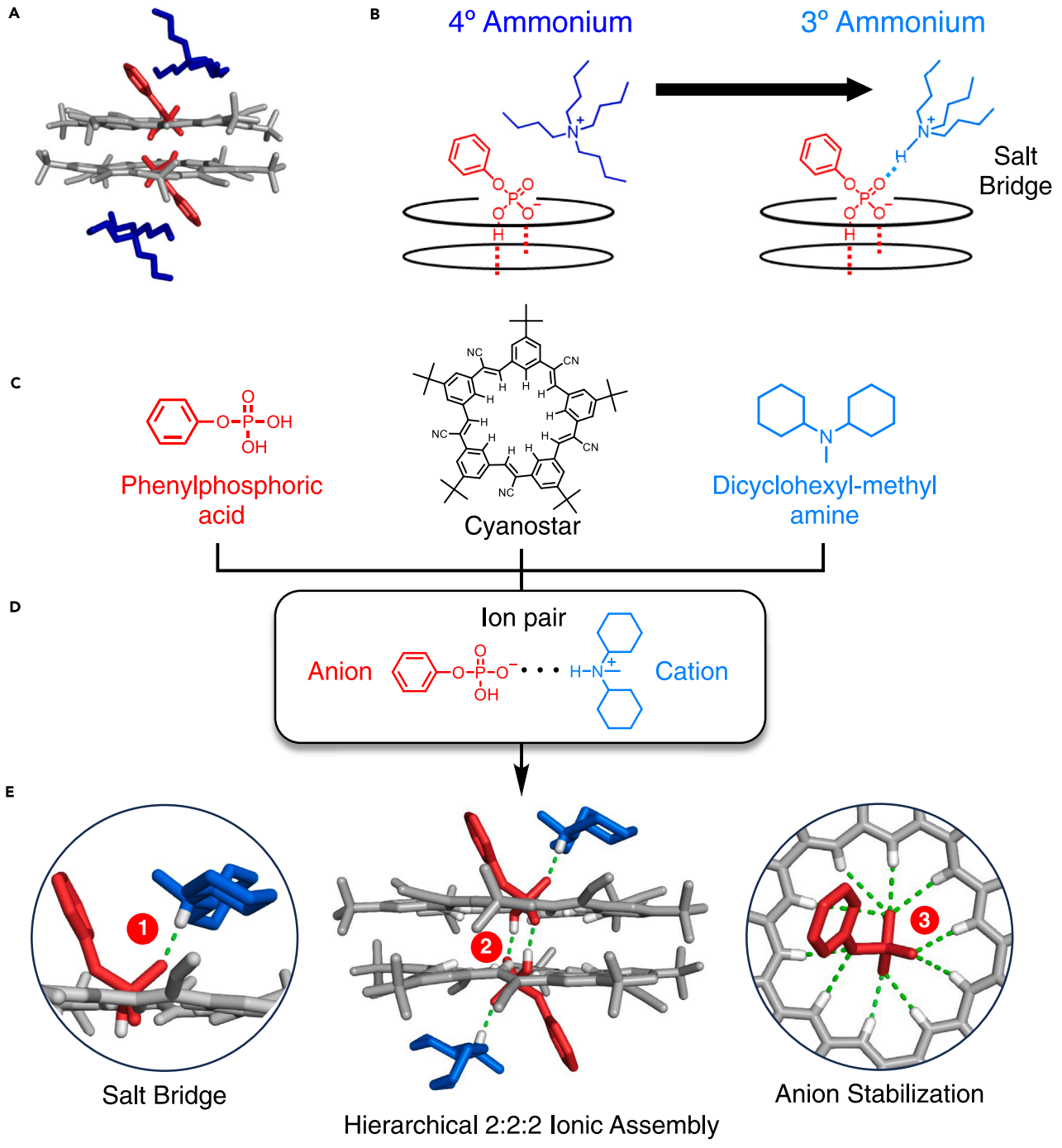

Figure 1. Formation of hierarchical ionic assembly by leveraging proton transfer between acid and amine for forming salt bridges

(A and B) (A) Crystal structure of cyanostar, phenyl phosphate, and 4° TBA^+ cations (CCDC# 2312047) providing inspiration for (B) replacing 4° cations with H-bonding 3° cations to form salt bridges.

(C and D) (C) Cyanostar mixed with phenyl phosphoric acid and dicyclohexyl-methyl amine undergoes (D) proton transfer to form the anion and cation capable of hierarchical formation of a 2:2:2 assembly (CCDC# 2312046) showing (1) NH, (2) OH, and (3) CH H-bonding.

common in solids[37,38,39,40] but rare[41] in solution. The H-bonding also turns on ion pairing in the building blocks (Figure 1D). It is not clear; therefore, whether the NH H-bonds will favor or disfavor product assembly. We explore these ideas by docking 3° ammonium cations with the privileged 2:2 complexes[42] that are formed between cyanostar macrocycles and

Please cite this article in press as: Chen et al., Diversifying hierarchical ionic assembly by docking cations to anions as salt bridges, Chem (2024), https://doi.org/10.1016/j.chempr.2024.07.005

organo-phosphate/-phosphonate anions. We find that the 2:2 complex is stable enough to support salt bridges with the cations and that the yield of assembly is controlled by solvent and sterics. We show how mixing bases, acids, and cyanostar allows the formation of 2:2:2 assemblies (Figures 1C–1E) and that the 82 examples explored herein open access to a new layer of diversity and structural ordering in hierarchical ionic assembly.

Use of 3° ammonium cations offers simplicity and scope to hierarchical anion assembly. The cations and associated anions can be made by proton transfer[43,44] upon adding 3° amines to acids with pK_a differences exceeding 4,[45] e.g., mixing 3° amines (pK_a ~11) with phenyl phosphoric acid (pK_{a1} ~2) allows preparation of the ionic assembly partners. Diversity arises from the variety of 3° amines available, ~3,000 from commercial suppliers alone. Generation of the same diversity with 4° cations using synthetic preparation[46,47] is a bottleneck for studying self-assembly. By contrast, use of proton transfer between amine and acid allows the numbers of salts to increase both quickly and reliably, e.g., mixing 9 amines and 8 acids reliably produces 72 combinations in quantitative yields. These numbers also allow use of high-throughput screening, which remains rare in the study of supramolecular systems.[48,49,50,51,52] These screens have the potential for identifying building blocks that form assemblies in high yield from a broad chemical space and help probe the underlying features controlling assembly.

Use of acid-base reactions to make ions and provide ionic stabilization to molecular recognition[53] and assembly[54] is not new. Early studies in anion recognition using polyaza receptors[41,55] formed complexes with ammonium H-bonds to anions. Salt bridges[53,56] that were studied early on,[57,58] e.g., amidinium carboxylate,[32] have now been extended to assembly.[59,60] Topical uses[61] involve CO_2 capture where its conversion to carbonic acid promotes proton transfer to an *N*-basic receptor rendering it cationic for binding HCO_3^- and crystallization. The inverse has been used for amine recognition. Therein, pre-incorporation of carboxylic acids into hosts facilitates proton transfer to amine guests and formation of an ionic complex.[53,62,63] Pre-incorporation of acidic or basic sites is believed[53] to be a simple way to associate two ionic partners rather than trying to assemble three components while avoiding competition from ion pairing. The rarity of examples where acid, base, and receptor are mixed to assemble into a single ionic species attests to this sentiment.

We present 82 examples where three charge-neutral components (receptor, acid, and amine) are mixed to undergo proton transfer and assemble into a 2:2:2 receptor-anion-cation species. We were inspired to replace the TBA^+ cations observed in crystal structures[64,65] formed between π-stacked cyanostars and a dimer of phenyl phosphates (Figure 1A) with 3° ammonium cations. We reasoned that the exposed oxygen atoms from the phosphate dimers could serve as docking sites for the cations (Figure 1B), but only if the 2:2 complex at the core was retained. Therein, phosphate dimers are partially stabilized by OH···O H-bonds.[65,66,67,68,69] These are described as anti-electrostatic H-bonds[70] on account of bringing two anions together against the dictates of Coulomb's law. A potential failure mode of assembly is therefore competition from stable, Coulomb-compliant ion pairs (Figure 1C).[43,44,53,71,72,73,74] This account describes both types of outcomes and how the simple preparation of diverse anions and cations allows for screening to identify privileged partners that undergo quantitative assembly. We screened 19 *N*-bases (12 amines, 7 heterocycles; Figure 2) including ditopics for polymerization,[75] piperidine and analogs common in drugs,[76] as well as the antidepressant Cipralex (escitalopram, ranked #188 by sales in 2022)[77] and prostate cancer therapeutic Zytiga (abiraterone acetate, ranked #51 by sales in 2022),[77] fluorescent compounds, quinolines used in photocatalysis,[78] and imidazoles used in ionic liquids[73] and as a buffer (pK_a 6.95). We contrast these outcomes to conventional 4° ammonium cations, like TBA^+, which have more reliable assembly and can also offer a source of diversity but only after clearing synthetic bottlenecks.[46] This work outlines how both anions and cations, instead of just one of them, can be tuned to enable the creation of desired assemblies by high-throughput screening as well as traditional synthetic design.

RESULTS AND DISCUSSION

To test our idea, we mixed cyanostar with phenyl phosphoric acid and dicyclohexyl-methyl amine in a stochiometric amount. The amine was selected because its protonated cation is soluble in a variety of organic solvents. The acid was selected based on our confidence in its ability to form a 2:2 complex.[65] A crystal structure (Figure 1E) shows formation of the 2:2:2 hierarchical assembly held together with three types of hydrogen bonds. At the center is the anion dimer connected by a pair of strong and self-complementary OH···O hydrogen bonds ($d_{O\ldots O}$ = 2.5 Å). The cyanostar dimer stabilizes the doubly charged anion dimer with 20 non-traditional CH···O hydrogen bond donors. The third layer of organization involves the charge-balancing ammonium cations that are connected to the accessible oxygen atoms of the anion dimer by N^+–H···O^- salt bridges ($d_{N\ldots O}$ = 2.7 Å).

The H-bonded anion-cation contacts are classified as salt bridges.[56] These bridges involve a hydrogen bond between the specific atoms believed to serve as the seat of the formal ionic charges. In the crystal structure we used for inspiration,[65] the oxygen atom in question is sp^2 hybridized and participates in a P=O double bond. Consistently, this bond is shorter (1.46 Å) than the P–O^- single bond (1.52 Å) involved in OH···O^- hydrogen bonding. However, in the 2:2:2 assembly formed with the 3° cation (Figure 1E), the phosphorous-oxygen bond lengths approach each other at 1.48 and 1.50 Å, respectively. These changes indicate that the 3° ammonium cation polarizes the phosphate, shifting charge density away from the center of the anion dimer such that it is now shared more evenly across the two oxygen atoms. The charge on the accessible oxygen acceptor atom is close to −0.5, and we can classify the association with the cation as a H-bonded salt bridge.

A key test for stability is whether the assembly remains intact when dissolved in solution. This stability is observed when the three components are mixed together in deuterated dichloromethane in an equimolar ratio (Figure 3). Specifically, signatures for the CH, OH, and NH H-bonds are observed in the ^{1}H NMR spectra (Figure 3).

Signatures of the receptor-anion pair at the heart of the assembly are observed in the ^{1}H NMR spectrum. The four aromatic

Please cite this article in press as: Chen et al., Diversifying hierarchical ionic assembly by docking cations to anions as salt bridges, Chem (2024), https://doi.org/10.1016/j.chempr.2024.07.005

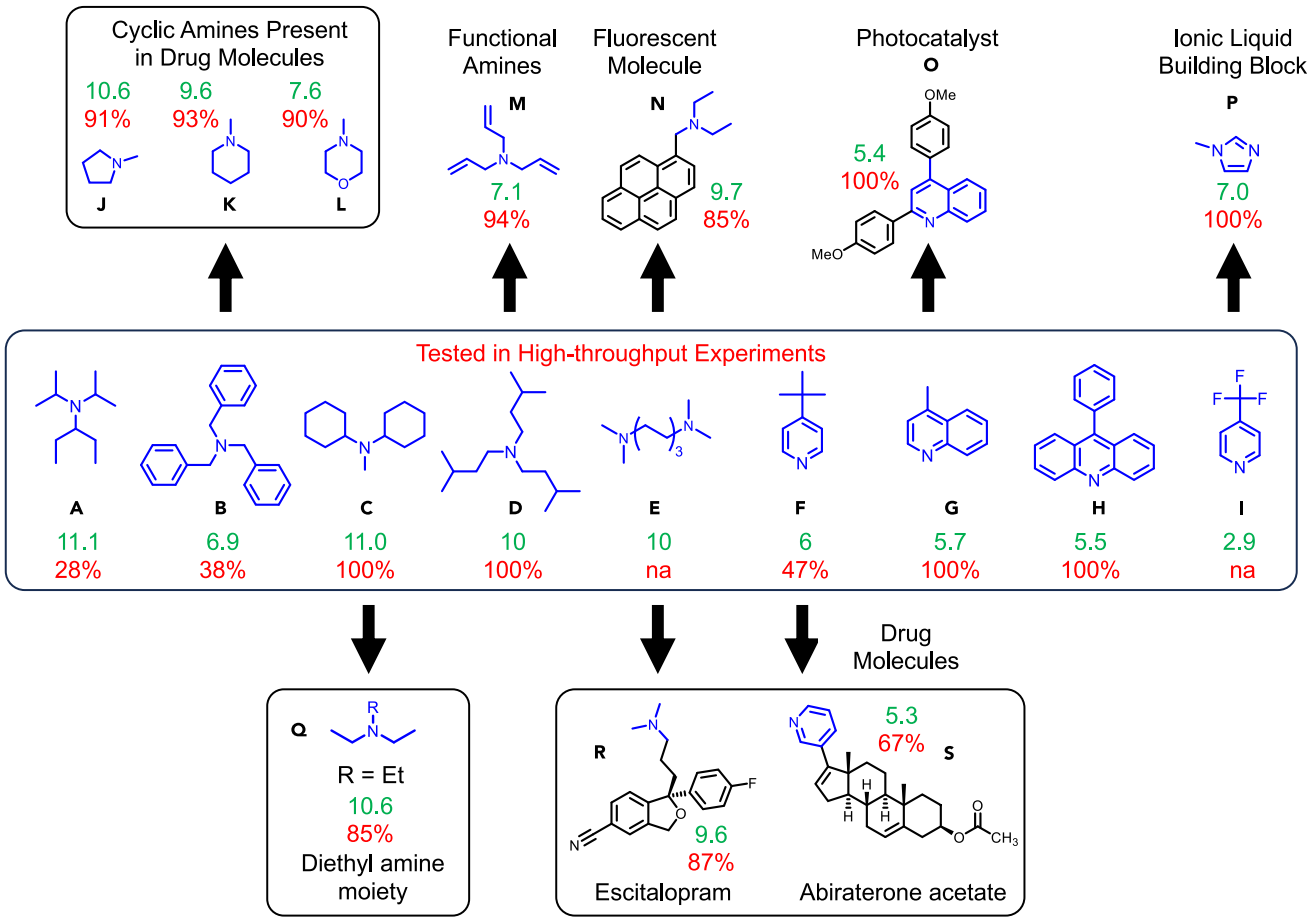

Figure 2. Diverse *N*-bases used in this work

Variety of 19 amines and *N*-heterocyclic bases tested in this study to explore a diverse set of building blocks. The pK_a values are listed in green and yields of co-assembly with phenyl phosphate anion and the cyanostar are listed in red.

peaks of the cyanostar double to generate an eight-line pattern characteristic of the π-stacked cyanostar dimer as described elsewhere.[65] These eight peaks correspond to the emergence of diastereomers defined by *meso* (68%) and *chiral* (32%) combinations of pairs of cyanostars. Formation of CH H-bonds from the cyanostar to the anion dimer is seen in the ~0.7-ppm downfield shifts of cavity protons H^a and H^d. We also observe the protons at the center of the anti-electrostatic hydrogen bond[65] in their typical position around 15 ppm and split into diastereomeric combinations. Their 15.1-ppm position is upfield relative to the 2:2:2 assembly formed with the TBA^+ cation (15.4 ppm),[65,79] indicating that the OH•••O H-bond is slightly weaker when assembled with the 3° cation. This interpretation is consistent with the longer O•••O distance seen with the 3° ammonium (2.50 Å) compared with the 4° TBA^+ cation (2.45 Å) and the equalization of charge across the phosphate that is induced by the cation.

Direct evidence for the NH hydrogen bond in the salt bridge is observed from the peak at 9.2 ppm. This peak was seen across many of the acid-amine combinations examined (Figures S1–S16). It is often shifted upfield relative to those seen in the spectra of the ion pairs alone (12.0 ppm, Figure S4). The chemical shift positions of the OH, NH, and CH hydrogen-bonded protons in the 2:2:2 assembly follow a rank order expected for their relative strengths (strong, medium, weak).[47]

The diffusion NMR (Figures 3 and S20) provides independent verification that the ternary assembly is formed in solution. Therein, all three components have the same diffusion coefficient ($D = 5.4 \pm 0.3 \times 10^{-10}$ m^2 s^{-1}). Thus, the 2:2:2 assembly seen in the crystals is the single unitary species present in solution.

Although these studies emphasize the amines, the underlying reliance on the acid-base reaction required for salt formation also adds diversity to the anion. To explore this idea, we examined organo-phosphonic acids in place of phosphoric acid (Figures S5–S16). We used 4-trifluoromethylphenyl vinyl phosphonic acid (CF_3-phenyl-VPA).[30] Its corresponding phosphonate co-assembles with cyanostar as a TBA^+ salt to form a central complex in which the oxygen atoms are exposed and available for H-bonding to 3° ammonium cations. It has a comparable acidity (pK_{a1} = 2.1) to facilitate the requisite proton transfer. Despite these similarities, an equimolar mixture of the three

Please cite this article in press as: Chen et al., Diversifying hierarchical ionic assembly by docking cations to anions as salt bridges, Chem (2024), https://doi.org/10.1016/j.chempr.2024.07.005

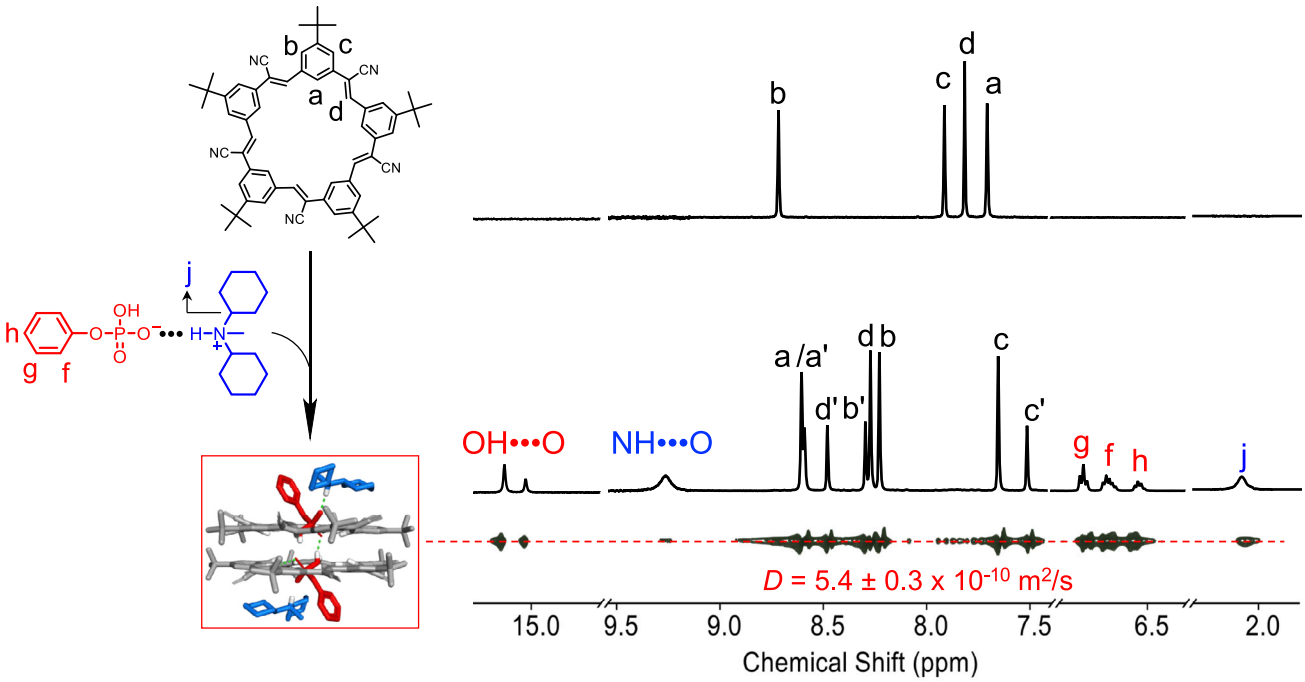

Figure 3. NMR characterization of 2:2:2 assembly

^{1}H NMR spectra of 2:2:2 ternary assembly formed from an equimolar mixture of phenyl phosphoric acid, dicyclohexyl-methyl amine, and cyanostar. Diffusion ordered spectroscopy (DOSY) data of the ternary assembly. (10 mM, CD_2Cl_2, 600 MHz, 298 K).

ingredients using the triisopentylamine instead generates a mixture of product and non-assembled starting materials (Figure 4A). We observe signals for the 2:2:2 species (black dots) corresponding to a 41% yield. Signals for the reactants include four aromatic peaks for the free cyanostar (black open circles) and weak peaks for the ion pair stemming from the phosphonate at 7.45 ppm (red open circles). Addition of excess ion pairs (2.5 equiv) helps drive formation of the 2:2:2 assembly. We also observe the H-bond signal at 12.25 ppm (blue open circle) for the excess ion pair. The presence of unique spectral signatures for the product and reactants provides the opportunity to better understand the equilibrium between ion pair and assembly (Figure 4B).

For direct comparison with the exemplary phosphate assembly (Figure 1), we combined the phosphonic acid with dicyclohexyl-methyl amine and cyanostar. We found that several factors change the position of equilibrium including temperature, concentration, addition of tetrabutylammonium chloride (TBACl), and solvent (Figures S25–S35). Among these, solvent has the most dramatic impact, allowing us to tune the yield between 0% and 100%. Changing the solvent from dichloromethane to a 3:1 mixture of dichloromethane and acetonitrile increases the proportion of 2:2:2 species from 52% to 100% (Figure S30), whereas use of tetrachloroethane decreases the yield to 0% in favor of the ion pair (Figure S27). Addition of small amounts of water, e.g., 0.5 μL, to the 3:1 mixture of dichloromethane and acetonitrile (540 mL) led to formation of the 2:2:2 complex with the cation dissociated in solution (Figure S30).

As a result of these sensitivity studies, we find that the phosphates regularly form stable 2:2:2 assemblies in dichloromethane whereas the phosphonates require a more polar solvent mixture (56:44 dichloromethane-to-acetonitrile)[80] to achieve similar outcomes.

High-throughput screening

In order to access the diversity represented by the ~3,000 commercially available 3° amines, we conducted high-throughput screening. We limit these studies to a proof-of-concept demonstration to prototype the method and evaluate its viability. We examined 72 combinations formed by mixing 9 commercially available amines and *N*-bases (a–i, Figure 5) with 8 acids of commercial or synthetic origins (1–8, Figure 5) and combining them with cyanostar in equimolar ratios. The four phosphoric acids and four phosphonic acids we selected cover a range of steric profiles[65] and include two ditopic acids capable of forming supramolecular polymers[79] (Figure S36). Pure dichloromethane is used with phosphoric acids to maximize the opportunity for identifying acid-amine partners that support high-fidelity assembly. Similarly, a 56:44 dichloromethane-acetonitrile mixture (*vide supra*) is used for the phosphonic acids. The 9 bases were selected to include diverse aliphatic amines and aromatic skeletons, a range of pK_a values spanning 2.9–11.1, and different steric profiles (Figures S37 and S38).

Across the 72 combinations (Figures S39–S110), we assign the yields of formation of the 2:2:2 assembly using NMR spectra (Figures S111–S190) and color code them accordingly. Of the 72 entries, the 50 colored green correspond to a heatmap for the

Please cite this article in press as: Chen et al., Diversifying hierarchical ionic assembly by docking cations to anions as salt bridges, Chem (2024), https://doi.org/10.1016/j.chempr.2024.07.005

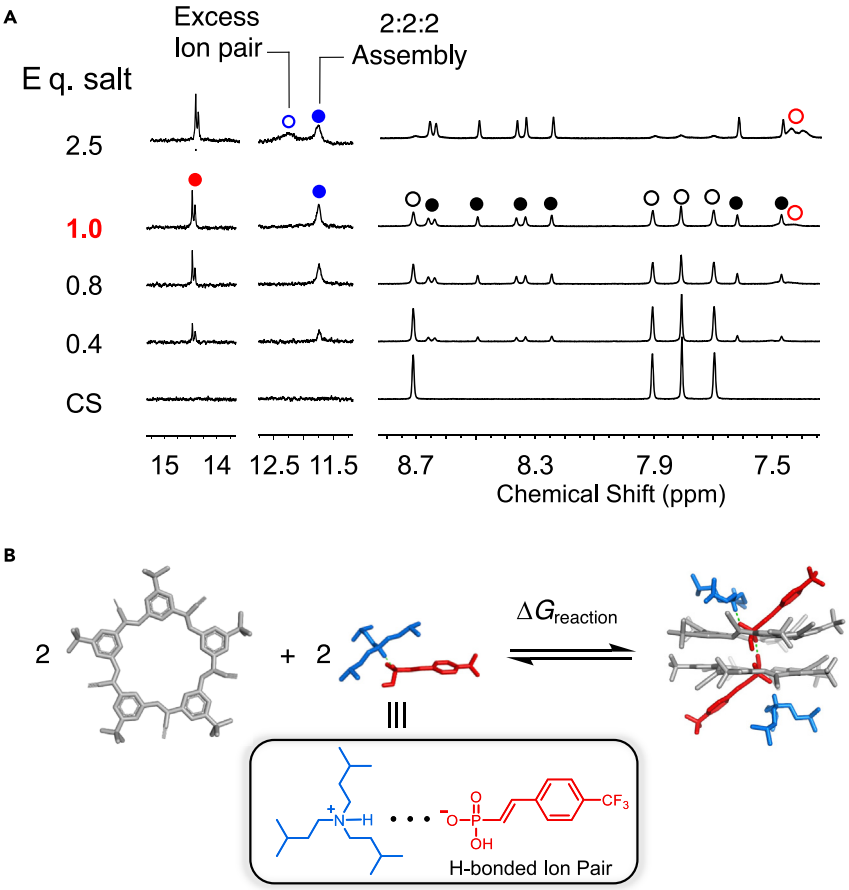

Figure 4. Equilibrium between reactants and the 2:2:2 assembly products

(A) ^{1}H NMR titration of the ion pair formed between triisopentyl ammonium and 4-trifluoromethylphenyl vinyl phosphonate into cyanostar (1 mM, CD_2Cl_2, 298 K, 600 MHz). Black solid circles are cyanostar dimers, empty circles are the free cyanostar. Red solid circles indicate OH H-bond and red empty circles indicate signals of excess phosphonate. Blue solid circles indicate NH H-bond in 2:2:2 assembly and the empty blue circle indicates H-bond in ion pair.

(B) Equilibrium between reactants composed of the ammonium-phosphonate ion pair and free cyanostar and the 2:2:2 assembly products.

degree of formation of the 2:2:2 species. Dark through light green corresponded to 100% through to low degrees of assembly (16%–74%). We used intensities of the OH···O signal (~15 ppm) and/or the 8-line signature of the CH···O protons in the aromatic region as indicators of the 2:2:2 species. This product signature is inversely correlated with the reactants, which are reflected in the four lines for the free cyanostar peaks. The NH peak for the 2:2:2 assembly has variable intensity, suggesting it is not a reliable marker for either the assembly or ion pair.

The 12 yellow entries are classified from the observation of 100% free cyanostar peaks. The 10 gray entries show either some degree of precipitation or ambiguous proton patterns not associated with either cyanostar dimers or free cyanostar.

We observe 13 combinations with quantitative formation of the target ternary assembly, indicating a 19% success rate. Phosphates favor assembly more than phosphonates and have a higher success rate of 28%. These 13 high-fidelity combinations represent a privileged set of receptor-anion-cation assembly partners. They include rigid cyclohexyl and flexible isopentyl substituents as well as bulky but rigid quinoline and acridine aromatics. Their structural and functional diversity provide multiple avenues for further exploration (*vide infra*).

In this screen, preparation of the salts and assemblies (2 days) took about the same time as the collection and analysis (2 days) of the ^{1}H-NMR spectra. By contrast, we estimate[46] that 72 salts using 4° ammonium cations would take 3–5 months to prepare. Thus, expedient acid-base preparation removes synthetic bottlenecks to reveal a bottleneck involving interpretation of the results, which is ongoing. Our preliminary findings are given next.

Interpretation of the screening results for ionic assembly

From the yellow entries composed of *p*-trifluoromethylpyridine (column **I**, pK_a = 2.92), the difference in acidity is not large enough to allow proton transfer with any of the acids (pK_{a1} ~2).[45] Success with pyridines (pK_a 5–6) show that pK_a differences exceeding 3 are viable for assembly.

The ditopic phosphate (row **4**) displays the signature of the 2:2:2 assembly with several cations to help lay a foundation for formation of supramolecular polymers. The ditopic amine (column **E**) also has the potential for polymerization; however, it yields precipitation, and further investigation is warranted.

We also observe the OH···O H-bond signature from a 3:2 cyanostar:anion assembly present as a minor species when combining alkyl-phosphoric acid **1** with amines **C** and **D**. This observation is consistent with a previous account[65] that the small size of the alkyl substituent on the phosphate allows generation of a triple stack of macrocycles. The extra macrocycle stabilizes the anion dimer and introduces steric bulk that will disfavor further assembly with cations. Despite this situation, this and other species may be alternative targets of optimization using acid-base screening.

Some combinations indicate that the amine's sterics play a role in controlling the yield of assembly. For instance, tribenzyl amine (**B**) and dicyclohexyl-methyl amine (**C**) display different degrees of assembly in the presence of phosphonic acid **6**. When combined with dichloromethane, we observe 0% and 75% yields of the corresponding 2:2:2 assemblies (Figure S33). To investigate the steric origin of these differences, we generated molecular models of the 2:2:2 complexes. For this purpose, we used molecular mechanics as an expedient way to evaluate the idea. Briefly, we used the 2:2 complex formed between anion

Please cite this article in press as: Chen et al., Diversifying hierarchical ionic assembly by docking cations to anions as salt bridges, Chem (2024), https://doi.org/10.1016/j.chempr.2024.07.005

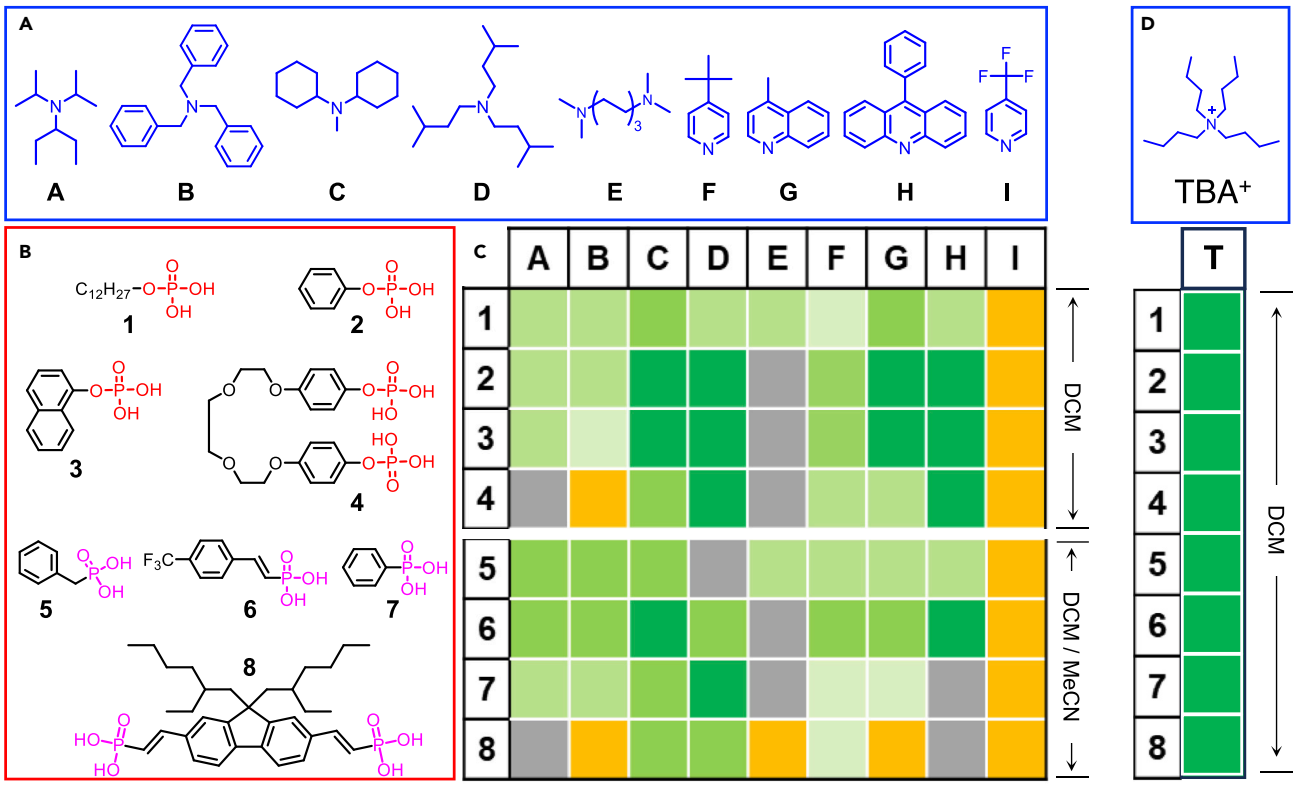

Figure 5. High-throughput experimentation using 72 different combinations of acids and amines

(A and B) (A) Amines and *N*-heterocyclic bases listed **A** to **I** and (B) acids numbered **1** to **8**.

(C) The dark green indicates 100% yield of ternary assembly, other gradations of green indicate varying degrees of assembly (16%–74%), the yellow indicates 100% free cyanostar and gray indicates precipitation or ambiguous NMR spectra. All samples at 1.6 mM in dichloromethane (**1**–**4**) or 54:44 dichloromethane-acetonitrile (**5**–**8**).

(D) Combination of the 4° TBA^+ cation with anions **1**–**8**.

$\mathbf{6}^-$ and cyanostar and then froze the geometry in the one obtained from the crystal structure.[30] We docked the two cations, $\mathbf{B}H^+$ and $\mathbf{C}H^+$, to the 2:2 complex and constrained the NH•••O bond distance (2.7 Å) to the one observed in the crystal of the 2:2:2 assembly (Figure 1E). In both cases, the three substituents on the cation need to be rotated away from the NH donor to expose it for H-bonding and to minimize steric contacts. The conformation of this H-bonded cation was optimized subject to these constraints, excised from the assembly, and its energy calculated. The geometry of the ion pair was also optimized but without constraints. The cation was again excised, and the energy of its conformation calculated (Figures S34 and S35). We evaluated the strain energy associated with changing the geometry of the cation in the ion pair (reactant) to the one in the 2:2:2 assembly (product). Consistent with a lower degree of assembly, we observed that a greater strain energy (102 kJ mol^{-1}) is necessary with cation $\mathbf{B}H^+$ compared with cation $\mathbf{C}H^+$ (55 kJ mol^{-1}). Similar effects were noted by McNally et al.[81,82] looking at the stabilities of ion pairs between ammonium and various anions.

These experiments also revealed cross-dependencies such that 100% assembly depends not only on the structure of the cation but also on its combination with specific anions. Combinations **C6** and **D7** have 100% yields, suggesting **C7** and **D6** would also favor assembly. However, their yields are 50% or less. Cooperativity between assembly partners must also be at play.

For the fluorescent acridinium cation (**H**) formed after proton transfer, we observe different fluorescence outcomes (pale green, yellow, green, and turquoise) when changing from acid **1** to acid **4** and examined under UV (Figure S191). These observations indicate the potential for environmentally responsive behaviors in the future.

We also examined triethylamine (TEA, Figure 2) on account of the simplicity with which the diethylamine moiety [$-NEt_2$] can be introduced into various building blocks by alkylation.[83,84,85,86,87,88,89] TEA also supports high-fidelity formation of the ternary assembly when combined with phenyl phosphate and cyanostar (Figure S24). Inspired by this example, we synthesized a diethylamino-functionalized pyrene (**N**) using *N*-alkylation. This amine was observed to co-assemble with phenyl phosphoric acid and cyanostar to afford the ternary assembly (85%). This promising result opens a pathway to deliver various functionalities to these 2:2:2 assemblies by synthetic design.

We took advantage of observations obtained from high-throughput experiments as well as the molecular skeletons to expand the diversity of amines (Figure 2) for ternary assembly.

Please cite this article in press as: Chen et al., Diversifying hierarchical ionic assembly by docking cations to anions as salt bridges, Chem (2024), https://doi.org/10.1016/j.chempr.2024.07.005

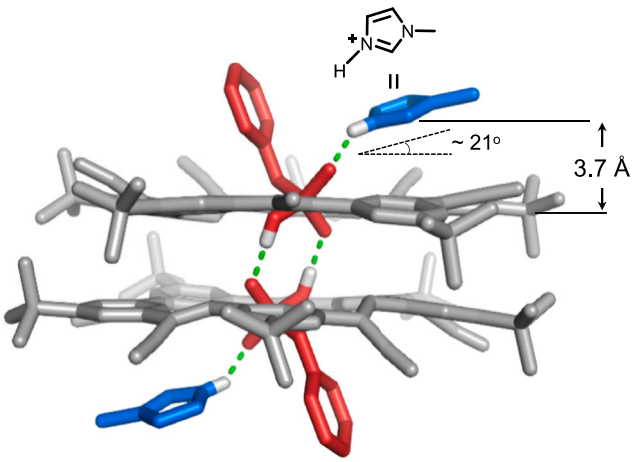

Figure 6. Crystal structure of the 2:2:2 assembly consisting of 1-methyl imidazolium, phenyl phosphate and cyanostar (CCDC# 2352315)

Green dashed lines indicate OH and NH hydrogen bonds.

To simplify assessments, we used phenyl phosphoric acid in all cases (Figures S219–S237). We expanded the scope of the amines to cyclic ones that are ubiquitous in pharmaceutical chemistry[76] including 1-methylpyrrolidine (**J**), 1-methylpiperidine (**K**), and 4-methylmorpholine (**L**) with assembly yields of 91%, 93%, and 90%, respectively. Triallylamine **M**, bearing free alkene groups ready for further modification using olefin metathesis, undergoes assembly (94%). We used a reported quinoline photocatalyst[78] **O** and found that it forms a high-fidelity ternary assembly (100%). We observed that imidazole, with wide use across various areas of ionic liquids, *N*-heterocyclic carbene synthesis, and as pH buffers, also assembles with 100% yield. The 2:2:2 crystal structure shows the imidazolium π stacking with the cyanostar at a distance of ~3.75 Å and titled 21° from the macrocycle's mean plane (Figure 6). Finally, drug molecules escitalopram (**R**) and abiraterone acetate (**S**) bearing trimethylamine or pyridine moieties, respectively, support the ternary assembly with 87% and 67% yields. The lower yield from **S** likely originates from its large steroidal structure. Thus, we have explored the diversity of options to include 10 unique compound classes offering broad access to areas spanning chemistry, materials, and biology. This demonstration of diversity shows the promising future of this simple assembly methodology.

Our studies with 1° and 2° amines show that they do not currently support formation of 2:2:2 species (Figures S192–S200). For these tests, we selected phenyl phosphoric acid (**2**) and the CF_3-phenyl-VPA (**6**) for combination with 1° and 2° amines, respectively. After acid-base reaction, the salts have poor solubility in dichloromethane as noted by Shinkai[31] Amines with longer alkyl chains, e.g., changing the alkyl from dibutylamine to didodecylamine, show modest improvements. We attribute these observations to stronger ion pairing and multiple NH hydrogen bonds.[43,72] The highest percentage of assembly is ~20% when the soluble salt of phenyl phosphate and didodecyl ammonium is combined with cyanostar. These observations suggest that two or more H-bonds in the ion pair are sufficient to outcompete formation of the assembly.

Comparison and scope for assembly with 4° ammonium cations

Motivated by these studies, we re-examined the aprotic 4° TBA^+ cation and compared it with the 3° cations formed by acid-base chemistry. Previous work with organophosphates[65] had found the TBA^+ to be dissociated from the 2:2 assemblies, but we recognized that use of a more polar medium (2:1 CD_2Cl_2:CD_3CN) likely promoted that outcome.[65] The diffusion ordered spectroscopy (DOSY, Figure S251) of the assembly formed upon mixing cyanostar with phenyl phosphate as the TBA^+ salt in dichloromethane show each component has the same diffusion coefficient. Thus, the 2:2:2 species is also formed with the 4° TBA^+ cation in dichloromethane.

The TBA^+ cation is routinely used to disfavor ion pairing and promote anion complexation. Thus, we expect its 2:2:2 assembly to be more stable relative to the ion pairs than what is possible with 3° ammonium cations. Using a competition study (Figure S243) with a 1:1 mixture of dicyclohexyl-methyl ammonium and TBA^+ as phenyl phosphate salts, we observe ^{1}H-NMR peak shifts that slightly favor assembly with the 4° TBA^+ cation. The resulting 60:40 ratio indicates a small energy difference of 1 kJ mol^{-1} (Figure S248).

These findings promote consideration of 4° ammonium and other aprotic cations as additional sources of chemical diversity. Our exploration of small-molecule, ionic isolation lattices[9] (SMILES) and the charge-by-charge assemblies[7,10] of Maeda using anion salts of cationic dyes also suggests the scope for ionic assembly is broader than considered with the 3° ammonium cations alone. To this end, we added a new column to the screen (Figure 5D) to highlight this possibility.

One key difference between 3° and 4° ammonium cations is their synthetic preparation. Use of 3° ammonium cations allows acid-base chemistry to add new combinations reliably and without fuss. The salts produced by acid-base chemistry do not require any special synthetic methods and rely on simple mixing and vacuum drying. Although they may be recrystallized to remove any residual acid or amine and raise purities, they are not necessarily any different than most commercial supplies that offer >98% purity. By contrast, the synthesis of 4° cations[46] requires *N*-alkylation of 3° amines and metathesis to access diverse combinations. The time investments needed for identifying reaction and purification conditions inhibit screening and investigations of how the cation's structure impacts the final assembly. However, these investments need not be prohibitive. Rather, the development of diverse 4° ammonium cations, possibly leveraging efforts in catalyst design[90] and the elaboration of other aprotic N^+-based cations, is expected to be a fruitful area of exploration.

Energetics of assembly

According to the different yields of 2:2:2 assembly when using the 3° and 4° ammonium cations, we can estimate the form of an energy profile of the system (Figure 7). The full energy landscape has been described with HSO_4^- forming 2:2:2 species.[64] In the present case; however, we are using the following

Please cite this article in press as: Chen et al., Diversifying hierarchical ionic assembly by docking cations to anions as salt bridges, Chem (2024), https://doi.org/10.1016/j.chempr.2024.07.005

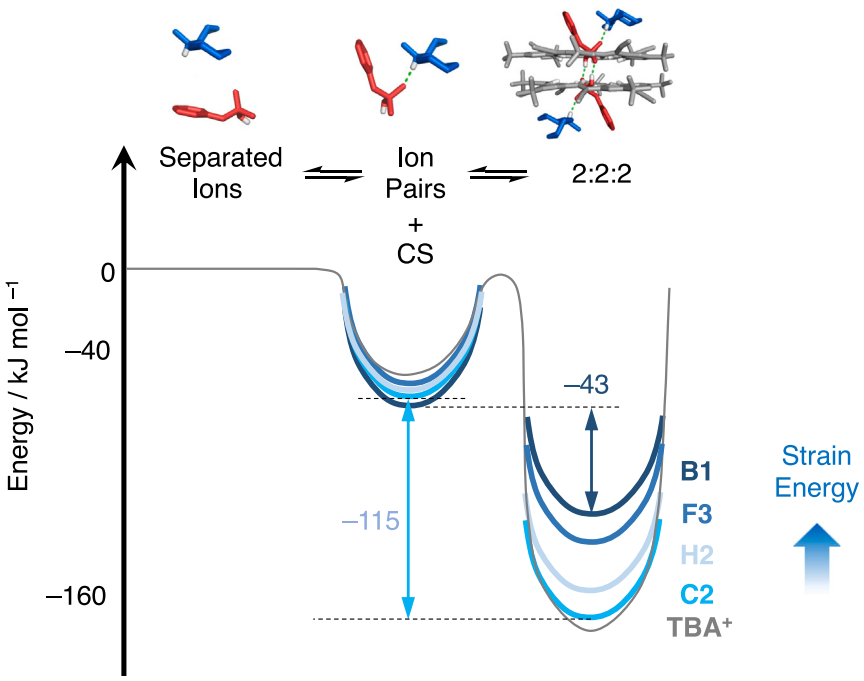

Figure 7. Schematic energy profile for assembly

Curves show estimates of the potential wells that describe the assembly of cyanostar with combinations of different organophosphate anions and nitrogen-based cations (blue curves). These are compared with the estimated curve for assembly with TBA-phenyl phosphate (gray curve). The reaction-free energies (ΔG_{rxn}/kJ mol^{-1}) are listed for **B1** and **C2** while relative ordering is provided for **F3** and **H2**.

estimates and assumptions. First, we measured the ion pairing (Figures S241 and S242) between TBA$^+$ and phenyl phosphate at −44 kJ mol^{-1} to help provide one anchor point for the energy profile for this cation (gray line, Figure 7). Second, ion pairing is believed to be stronger for the 3° ammonium cations[31] and depends on the identity[82] of anion and cation, leading to the energy spread shown in the blue wells for the salts of **B1**, **C2**, **F3**, and **H2**. Third, the 2:2:2 assembly using dicyclohexyl-methyl ammonium with phenyl phosphate (**C2**) is only slightly weaker (1 kJ mol^{-1}) than with TBA$^+$. Fourth, we use the 0%–100% populations to generate reaction-free energies ΔG_{rxn} (Figures S238–S240). These span from less than 0 kJ mol^{-1} to more than −115 kJ mol^{-1}.[91]

We observe a large range in the reaction-free energies of assembly. We believe that the variations in the energies of the products are bigger than in the reactants. One source of the difference between the reactants (ion pair and cyanostar) and product (2:2:2) is the additional strain energy in the cation needed for formation of the assembly (*vide supra*). We used the calculated strain energies on bulky **B**H$^+$ and compact **C**H$^+$ to situate the bottom of the energy wells of their 2:2:2 assemblies ~40 kJ mol^{-1} apart from each other. In addition, a competition study (Figure S252) suggests the 2:2:2 with aliphatic ammonium **C2** is more stable than aromatic **H2** by 3 kJ mol^{-1}. We believe that the strain energy is the biggest source of variation in both reaction-free energies and overall stabilities of the 2:2:2 assemblies. It follows; therefore, that stability depends on the identity of the 3° cation.

Conclusions

We used simple acid-base chemistry and stable anion-receptor complexes to provide access to chemically diverse ammonium cations for hierarchical ionic assembly. The 3° ammonium cations are observed to dock with the primary 2:2 cyanostar-anion assembly where the cations serve as a secondary layer of structural ordering in the hierarchical assembly. The ternary 2:2:2 assembly is in a competitive equilibrium with the simple 1:1 ion pair plus free cyanostar. This equilibrium depends on the stability of the anion-receptor complex at the core. Phosphates show a greater number of high-yield assemblies relative to phosphonates. The position of equilibrium is highly sensitive to the solvent used, with changes in polarity capable of turning assembly both on and off by favoring either the 2:2:2 assembly or ion pair. A high-throughput screen of 72 combinations was used to evaluate a diverse set of acids and bases and their corresponding ionized forms as anions and cations. We used the screening to rapidly identify 13 partners that produce the assembly in quantitative yields. We identified the diethylamine moiety, −NEt$_2$, as a functional group that can be conveniently introduced using high-yielding covalent chemistry, e.g., *N*-alkylation. Diversity was extended to cationic forms of photocatalysts, drug molecules, fluorophores, and a component of ionic liquids to demonstrate straightforward integration with other sub-fields of chemistry. The simplicity of preparation allows a manual NMR screening process to be conducted. The NMR output affords insight into the structural state of assembly and aids our understanding of molecule-level details, e.g., the effect of sterics and strain on yield. These studies also identified 4° ammonium cations as potential sources of diversity to explore in the future after removing synthesis bottlenecks. The systems presented are exemplary of the benefits accruing when diverse cations and anions are combined into a simple assembly pipeline to produce hierarchical molecules and materials. Future applications include the use of fluorescent materials and supramolecular polymers.

EXPERIMENTAL PROCEDURES

Resource availability

Lead contact

Further information and requests for resources should be directed to and will be fulfilled, where possible, by the lead contact, Amar H. Flood (aflood@iu.edu).

Materials availability

The experimental dataset and materials generated are available from the lead contact upon reasonable request.

Data and code availability

All data is available from the lead contact upon reasonable request.

Accession codes

CCDC 2312046, 2312047, and 2352315 contain the supplementary crystallographic data for this paper. These data can be obtained free of charge via www.ccdc.cam.ac.uk/data_request/cif, by emailing data_request@ccdc.cam.ac.uk, or by contacting The Cambridge Crystallographic Data Centre, 12 Union Road, Cambridge CB2 1EZ, UK; fax: +44 1223 336033.

SUPPLEMENTAL INFORMATION

Supplemental information can be found online at https://doi.org/10.1016/j.chempr.2024.07.005.

ACKNOWLEDGMENTS

This work was supported by the National Science Foundation (CHE-2105848). This work was authored in part by the National Renewable Energy Laboratory (NREL), operated by Alliance for Sustainable Energy, LLC, for the U.S. Department of Energy (DOE) under contract no. DE-AC36-08GO28308. Synthesis of the organophosphonic acids at Colorado School of Mines was funded by the Separation Science Program, Division of Chemical Sciences, Geosciences, and Biosciences (CSGB) Division, and the Physical Behavior of Materials Program, Materials Sciences and Engineering (MSE) Division, within the Office of Basic Energy Sciences, Office of Science, DOE, through the Materials and Chemical Sciences Research on Critical Materials National Laboratory Program (LAB 20-2304). The 500 MHz NMR spectrometer of the Indiana University NMR facility was supported by NSF grant CHE-1920026 and the Prodigy probe was purchased in part with support from the Indiana Clinical and Translational Sciences Institute funded, in part by NIH Award TL1TR002531. Support for the acquisition of the Bruker Venture D8 diffractometer through the Major Scientific Research Equipment Fund from the President of Indiana University and the Office of the Vice President for Research is gratefully acknowledged. Y.C. acknowledges the support from Slagle Fellowship. We thank the staff of the Indiana University Mass Spectrometry Facility for recording mass spectra. We thank Dr. Wei Zhao for sharing triethylene glycol bis(phenyl-*p*-phosphoric acid) for the high-throughput screening and Dr. Jianbin Li for sharing the photocatalyst. The views expressed in the article do not necessarily represent the views of the DOE or the US Government.

AUTHOR CONTRIBUTIONS

Project conceptualization, Y.C. and A.H.F.; formal analysis, Y.C.; resources, A.K.; investigation, Y.C., D.K., M.P., and V.C.; methodology, Y.C.; project administration, A.H.F.; writing – original draft, review & editing, Y.C.; writing – review & editing, D.K, A.K., M.P., V.C., A.S., and A.H.F.; supervision, A.S. and A.H.F.; funding acquisition, A.S. and A.H.F.

DECLARATION OF INTERESTS

A provisional patent has been submitted. A.H.F. is a member of the *Chem* advisory board.

Received: January 27, 2024
Revised: March 12, 2024
Accepted: July 10, 2024
Published: August 6, 2024

REFERENCES

1. Kim, S.K., and Sessler, J.L. (2010). Ion pair receptors. Chem. Soc. Rev. *39*, 3784–3809. https://doi.org/10.1039/c002694h.
2. He, Q., Vargas-Zúñiga, G.I., Kim, S.H., Kim, S.K., and Sessler, J.L. (2019). Macrocycles as Ion Pair Receptors. Chem. Rev. *119*, 9753–9835. https://doi.org/10.1021/acs.chemrev.8b00734.
3. Liang, L., Zhao, W., Yang, X.J., and Wu, B. (2022). Anion-Coordination-Driven Assembly. Acc. Chem. Res. *55*, 3218–3229. https://doi.org/10.1021/acs.accounts.2c00435.
4. Zhang, L., Li, B., Li, R., Wang, Y., Ye, S., Zhang, P., and Wu, B. (2023). Spontaneous Resolution of Chiral Janus-Type Double-Layered Metallocyclic Strips Incorporating Mobius Ring and Circular Helicate. J. Am. Chem. Soc. *145*, 18221–18226. https://doi.org/10.1021/jacs.3c05746.
5. Bai, X., Jia, C., Zhao, Y., Yang, D., Wang, S.C., Li, A., Chan, Y.T., Wang, Y.Y., Yang, X.J., and Wu, B. (2018). Peripheral Templation-Modulated Interconversion between an A4 L6 Tetrahedral Anion Cage and A2 L3 Triple Helicate with Guest Capture/Release. Angew. Chem. Int. Ed. Engl. *57*, 1851–1855. https://doi.org/10.1002/anie.201712080.
6. Li, B., Zhang, W., Lu, S., Zheng, B., Zhang, D., Li, A., Li, X., Yang, X.J., and Wu, B. (2020). Multiple Transformations among Anion-based $A_{2n}L_{3n}$ Assemblies: Bicapped Trigonal Antiprism A_8L_{12}, Tetrahedron A_4L_6, and Triple Helicate A_2L_3 (A = Anion). J. Am. Chem. Soc. *142*, 21160–21168. https://doi.org/10.1021/jacs.0c10346.
7. Haketa, Y., Sasaki, S., Ohta, N., Masunaga, H., Ogawa, H., Mizuno, N., Araoka, F., Takezoe, H., and Maeda, H. (2010). Oriented salts: dimension-controlled charge-by-charge assemblies from planar receptor-anion complexes. Angew. Chem. Int. Ed. Engl. *49*, 10079–10083. https://doi.org/10.1002/anie.201006356.
8. Haketa, Y., Bando, Y., Takaishi, K., Uchiyama, M., Muranaka, A., Naito, M., Shibaguchi, H., Kawai, T., and Maeda, H. (2012). Asymmetric induction in the preparation of helical receptor-anion complexes: ion-pair formation with chiral cations. Angew. Chem. Int. Ed. Engl. *51*, 7967–7971. https://doi.org/10.1002/anie.201202196.
9. Benson, C.R., Kacenauskaite, L., VanDenburgh, K.L., Zhao, W., Qiao, B., Sadhukhan, T., Pink, M., Chen, J., Borgi, S., Chen, C.-H., et al. (2020). Plug-and-Play Optical Materials from Fluorescent Dyes and Macrocycles. Chem *6*, 1978–1997. https://doi.org/10.1016/j.chempr.2020.06.029.
10. Haketa, Y., Komatsu, K., Sei, H., Imoba, H., Ota, W., Sato, T., Murakami, Y., Tanaka, H., Yasuda, N., Tohnai, N., and Maeda, H. (2024). Enhanced solid-state phosphorescence of organoplatinum pi-systems by ion-pairing assembly. Chem. Sci. *15*, 964–973. https://doi.org/10.1039/d3sc04564a.
11. Skala, L.P., Aguilar-Enriquez, X., Stern, C.L., and Dichtel, W.R. (2023). Dissipative crystallization of ion-pair receptors. Chem *9*, 709–720. https://doi.org/10.1016/j.chempr.2022.12.010.
12. Zhang, W., Jin, W., Fukushima, T., Saeki, A., Seki, S., and Aida, T. (2011). Supramolecular linear Heterojunction Composed of Graphite-Like Semiconducting Nanotubular Segments. Science *334*, 340–343. https://doi.org/10.1126/science.1210369.
13. Aida, T., Meijer, E.W., and Stupp, S.I. (2012). Functional Supramolecular Polymers. Science *335*, 813–817. https://doi.org/10.1126/science.1205962.
14. Yu, Z., Tantakitti, F., Yu, T., Palmer, L.C., Schatz, G.C., and Stupp, S.I. (2016). Simultaneous covalent and noncovalent hybrid polymerizations. Science *351*, 497–502. https://doi.org/10.1126/science.aad4091.
15. Kleine-Kleffmann, L., Stepanenko, V., Shoyama, K., Wehner, M., and Würthner, F. (2023). Controlling the Supramolecular Polymerization of Squaraine Dyes by a Molecular Chaperone Analogue. J. Am. Chem. Soc. *145*, 9144–9151. https://doi.org/10.1021/jacs.3c01002.
16. Wang, S., Huang, Z., Li, A., Zhao, Y., Zuo, W., Li, Y., Miao, H., Ma, J., Sun, W., Wang, X., et al. (2021). Crown Ether Functionalized Potassium-Responsive Anionocages for Cascaded Guest Delivery. Angew. Chem. Int. Ed. Engl. *60*, 9573–9579. https://doi.org/10.1002/anie.202100441.
17. Barbera, L., De Plano, L.M., Franco, D., Gattuso, G., Guglielmino, S.P.P., Lando, G., Notti, A., Parisi, M.F., and Pisagatti, I. (2018). Antiadhesive and antibacterial properties of pillar[5]arene-based multilayers. Chem. Commun. *54*, 10203–10206. https://doi.org/10.1039/c8cc05659e.

18. Hutskalov, I., Linden, A., and Čorić, I. (2023). Directional Ionic Bonds. J. Am. Chem. Soc. *145*, 8291–8298. https://doi.org/10.1021/jacs.3c01030.

19. Skala, L.P., Stern, C.L., Bancroft, L., Moisanu, C.M., Pelkowski, C., Aguilar-Enriquez, X., Swartz, J.L., Wasielewski, M.R., and Dichtel, W.R. (2023). A modular platform for the precise assembly of molecular frameworks composed of ion pairs. Chem *9*, 1208–1220. https://doi.org/10.1016/j.chempr.2023.01.011.

20. Moisanu, C.M., Jacobberger, R.M., Skala, L.P., Stern, C.L., Wasielewski, M.R., and Dichtel, W.R. (2023). Crystalline Arrays of Copper Porphyrin Qubits Based on Ion-Paired Frameworks. J. Am. Chem. Soc. *145*, 18447–18454. https://doi.org/10.1021/jacs.3c04786.

21. Yang, P., Wang, J., Jia, C., Yang, X.J., and Wu, B. (2013). Dinuclear Chloride-Binding Foldamers Based on Fluorescent Oligoureas. Eur. J. Org. Chem. *2013*, 3446–3454. https://doi.org/10.1002/ejoc.201300043.

22. Silver, E.S., Rambo, B.M., Bielawski, C.W., and Sessler, J.L. (2014). Reversible anion-induced cross-linking of well-defined calix[4]pyrrole-containing copolymers. J. Am. Chem. Soc. *136*, 2252–2255. https://doi.org/10.1021/ja4123895.

23. Caballero, A., Swan, L., Zapata, F., and Beer, P.D. (2014). Iodide-induced shuttling of a halogen- and hydrogen-bonding two-station rotaxane. Angew. Chem. Int. Ed. Engl. *53*, 11854–11858. https://doi.org/10.1002/anie.201407580.

24. Gavette, J.V., Evoniuk, C.J., Zakharov, L.N., Carnes, M.E., Haley, M.M., and Johnson, D.W. (2014). Exploring Anion-Induced Conformational Flexibility and Molecular Switching in a Series of Heteroaryl-Urea Receptors. Chem. Sci. *5*, 2899–2905. https://doi.org/10.1039/C4SC00950A.

25. Wang, H., Fang, S., Wu, G., Lei, Y., Chen, Q., Wang, H., Wu, Y., Lin, C., Hong, X., Kim, S.K., et al. (2020). Constraining Homo- and Heteroanion Dimers in Ultraclose Proximity within a Self-Assembled Hexacationic Cage. J. Am. Chem. Soc. *142*, 20182–20190. https://doi.org/10.1021/jacs.0c10253.

26. Sergeant, G.E., and Jolliffe, K.A. (2020). Anion recognition using a simple cyclic peptide. Supramol. Chem. *32*, 233–237. https://doi.org/10.1080/10610278.2020.1732377.

27. Zapata, F., González, L., Bastida, A., Bautista, D., and Caballero, A. (2020). Formation of self-assembled supramolecular polymers by anti-electrostatic anion-anion and halogen bonding interactions. Chem. Commun. *56*, 7084–7087. https://doi.org/10.1039/d0cc02831b.

28. Wezenberg, S.J., Chen, L.J., Bos, J.E., Feringa, B.L., Howe, E.N.W., Wu, X., Siegler, M.A., and Gale, P.A. (2022). Photomodulation of Transmembrane Transport and Potential by Stiff-Stilbene Based Bis(thio)ureas. J. Am. Chem. Soc. *144*, 331–338. https://doi.org/10.1021/jacs.1c10034.

29. Zhu, J., Sun, X.W., Yang, X., Yu, S.N., Liang, L., Chen, Y.Z., Zheng, X., Yu, M., Yan, L., Tang, J., et al. (2023). In Situ Photoisomerization of an Azobenzene-Based Triple Helicate with a Prolonged Thermal Relaxation Time. Angew. Chem. Int. Ed. Engl. *62*, e202314510. https://doi.org/10.1002/anie.202314510.

30. Chen, Y., Kuvayskaya, A., Pink, M., Sellinger, A., and Flood, A.H. (2023). A library of vinyl phosphonate anions dimerize with cyanostars, form supramolecular polymers and undergo statistical sorting. Chem. Sci. *15*, 389–398. https://doi.org/10.1039/d3sc03685e.

31. Sada, K., Tani, T., and Shinkai, S. (2006). Organic ammonium carboxylates as supramolecular building blocks: The role of ionic hydrogen bonding. Synlett *2006*, 2364–2374. https://doi.org/10.1055/s-2006-951469.

32. Sessler, J.L., Gale, P.A., and Cho, W.-S. (2006). Anion Receptor Chemistry (Royal Society of Chemistry).

33. Sessler, J.L., Gross, D.E., Cho, W.-S., Lynch, V.M., Schmidtchen, F.P., Bates, G.W., Light, M.E., and Gale, P.A. (2006). Calix[4]pyrrole as a chloride anion receptor: solvent and countercation effects. J. Am. Chem. Soc. *128*, 12281–12288. https://doi.org/10.1021/ja064012h.

34. Hua, Y., Ramabhadran, R.O., Uduehi, E.O., Karty, J.A., Raghavachari, K., and Flood, A.H. (2011). Aromatic and aliphatic CH hydrogen bonds fight for chloride while competing alongside ion pairing within triazolophanes. Chem. Eur. J. *17*, 312–321. https://doi.org/10.1002/chem.201002340.

35. Bowman-James, K. (2005). Alfred Werner revisited: the coordination chemistry of anions. Acc. Chem. Res. *38*, 671–678. https://doi.org/10.1021/ar040071t.

36. Kang, S.O., Llinares, J.M., Day, V.W., and Bowman-James, K. (2010). Cryptand-like anion receptors. Chem. Soc. Rev. *39*, 3980–4003. https://doi.org/10.1039/c0cs00083c.

37. Bell, R.A., Christoph, G.G., Fronczek, F.R., and Marsh, R.E. (1975). The cation H13O6+: a short, symmetric hydrogen bond. Science *190*, 151–152. https://doi.org/10.1126/science.190.4210.151.

38. Metz, B., Rosalky, J.M., and Weiss, R. (1976). [3] Cryptates: X-ray crystal structures of the chloride and ammonium ion complexes of a spheroidal macrotricyclic ligand. Chem. Commun. *14*, 533b–534. https://doi.org/10.1039/C3976000533B.

39. Hossain, M.A., Liljegren, J.A., Powell, D., and Bowman-James, K. (2004). Anion binding with a tripodal amine. Inorg. Chem. *43*, 3751–3755. https://doi.org/10.1021/ic049762b.

40. Mascal, M., Yakovlev, I., Nikitin, E.B., and Fettinger, J.C. (2007). Fluoride-selective host based on anion-pi interactions, ion pairing, and hydrogen bonding: synthesis and fluoride-ion sandwich complex. Angew. Chem. Int. Ed. Engl. *46*, 8782–8784. https://doi.org/10.1002/anie.200704005.

41. Lin, W., Zhang, G., Zhu, X., Yu, P., Alimi, L.O., Moosa, B.A., Sessler, J.L., and Khashab, N.M. (2023). Caging the Hofmeister Effect by a Biomimetic Supramolecular Receptor. J. Am. Chem. Soc. *145*, 12609–12616. https://doi.org/10.1021/jacs.3c01849.

42. Zhao, W., Qiao, B., Tropp, J., Pink, M., Azoulay, J.D., and Flood, A.H. (2019). Linear Supramolecular Polymers Driven by Anion-Anion Dimerization of Difunctional Phosphonate Monomers Inside Cyanostar Macrocycles. J. Am. Chem. Soc. *141*, 4980–4989. https://doi.org/10.1021/jacs.9b00248.

43. Basit, H., Pal, A., Sen, S., and Bhattacharya, S. (2008). Two-component hydrogels comprising fatty acids and amines: structure, properties, and application as a template for the synthesis of metal nanoparticles. Chem. Eur. J. *14*, 6534–6545. https://doi.org/10.1002/chem.200800374.

44. Montero de Espinosa, L., Balog, S., and Weder, C. (2014). Isophthalic Acid-Pyridine H-Bonding: Simplicity in the Design of Mechanically Robust Phase-Segregated Supramolecular Polymers. ACS Macro Lett. *3*, 540–543. https://doi.org/10.1021/mz500293x.

45. Shmukler, L.E., Fedorova, I.V., Gruzdev, M.S., and Safonova, L.P. (2019). Triethylamine-Based Salts: Protic Ionic Liquids or Molecular Complexes? J. Phys. Chem. B *123*, 10794–10806. https://doi.org/10.1021/acs.jpcb.9b08032.

46. (a) For nine 4° ammonium cations, we would require 9 N-alkylations, which could be run in 2 days. Each would require purification largely by trial and error at possibly a success rate of 3 per day for 3 days. Thus, 9 chloride salts could be prepared in 2 days. For the target organophosphate anions would need to be prepared by reaction of the acid with NaOH. The sodium and chloride salts could be used in a metathesis reaction facilitated by precipitation of NaCl to isolate the 4° ammonium salts of the phosphate of interest. Purification would be needed. The metathesis and purification would need to be conducted for each of the 72 target salts. Assuming the same rate of 3 purifications per day to total 24 days. The grand total would be 31 days or about 6 weeks. Given the typical factor of π as the ratio between how long something takes versus how long you expect it to take, the time frame to make 72 salts might take 4-5 months. (b) Alternatively, after preparation of the nine 4° ammonium cations as BF_4^- or Cl^- salts, they could be subject to metathesis with hydroxide to prepare the OH^- versions. These would be amenable to acid-base reaction with the organophosphoric acids. Thus, after the alkylations (2 days), a reliable method for hydroxide metathesis would be needed, perhaps established over 2 weeks (10 days). Then, it could be repeated at 3 per day totaling 3 days. Generation of the target 72 salts would then proceed as per the acid-base reactions used with acids and 3° amines explored herein

(2 days). The grand total would be 17 days factoring π to generate the 72 within 3 months.

47. Jeffrey, G.A. (1997). An introduction to hydrogen bonding (Oxford University Press).
48. Greenaway, R.L., Santolini, V., Bennison, M.J., Alston, B.M., Pugh, C.J., Little, M.A., Miklitz, M., Eden-Rump, E.G.B., Clowes, R., Shakil, A., et al. (2018). High-throughput discovery of organic cages and catenanes using computational screening fused with robotic synthesis. Nat. Commun. *9*, 2849. https://doi.org/10.1038/s41467-018-05271-9.
49. Cui, P., McMahon, D.P., Spackman, P.R., Alston, B.M., Little, M.A., Day, G.M., and Cooper, A.I. (2019). Mining predicted crystal structure landscapes with high throughput crystallisation: old molecules, new insights. Chem. Sci. *10*, 9988–9997. https://doi.org/10.1039/c9sc02832c.
50. Ollerton, K., Greenaway, R.L., and Slater, A.G. (2021). Enabling technology for supramolecular chemistry. Front. Chem. *9*, 774987. https://doi.org/10.3389/fchem.2021.774987.
51. Zhao, W., Yan, P., Li, B., Bahri, M., Liu, L., Zhou, X., Clowes, R., Browning, N.D., Wu, Y., Ward, J.W., and Cooper, A.I. (2022). Accelerated Synthesis and Discovery of Covalent Organic Framework Photocatalysts for Hydrogen Peroxide Production. J. Am. Chem. Soc. *144*, 9902–9909. https://doi.org/10.1021/jacs.2c02666.
52. Vijayakrishnan, S., Ward, J.W., and Cooper, A.I. (2022). Discovery of a Covalent Triazine Framework Photocatalyst for Visible-Light-Driven Chemical Synthesis using High-Throughput screening. ACS Catal. *12*, 10057–10064. https://doi.org/10.1021/acscatal.2c02743.
53. Gattuso, G., Crisafulli, D., Milone, M., Mancuso, F., Pisagatti, I., Notti, A., and Parisi, M.F. (2022). Proton transfer mediated recognition of amines by ionizable macrocyclic receptors. Chem. Commun. (Camb) *58*, 10743–10756. https://doi.org/10.1039/d2cc04047f.
54. Trivedi, D.R., Ballabh, A., Dastidar, P., and Ganguly, B. (2004). Structure–property correlation of a new family of organogelators based on organic salts and their selective gelation of oil from oil/water mixtures. Chem. Eur. J. *10*, 5311–5322. https://doi.org/10.1002/chem.200400122.
55. Llinares, J.M., Powell, D., and Bowman-James, K. (2003). Ammonium based anion receptors. Coord. Chem. Rev. *240*, 57–75. https://doi.org/10.1016/S0010-8545(03)00019-5.
56. Donald, J.E., Kulp, D.W., and DeGrado, W.F. (2011). Salt bridges: geometrically specific, designable interactions. Proteins *79*, 898–915. https://doi.org/10.1002/prot.22927.
57. Blondeau, P., Segura, M., Pérez-Fernández, R., and de Mendoza, J. (2007). Molecular recognition of oxoanions based on guanidinium receptors. Chem. Soc. Rev. *36*, 198–210. https://doi.org/10.1039/b603089k.
58. Dietrich, B., Fyles, T.M., Lehn, J.-M., Pease, L.G., and Fyles, D.L. (1978). Anion receptor molecules. Synthesis and some anion binding properties of macrocyclic guanidinium salts. J. Chem. Soc. Chem. Commun. *21*, 934–936.
59. Iida, H., Shimoyama, M., Furusho, Y., and Yashima, E. (2010). Double-Stranded Supramolecular Assembly through Salt Bridge Formation between Rigid and Flexible Amidine and Carboxylic Acid Strands. J. Org. Chem. *75*, 417–423. https://doi.org/10.1021/jo902158v.
60. Jiang, H., Xie, L., Duan, Z., Lin, K., He, Q., Lynch, V.M., Sessler, J.L., and Wang, H. (2021). Fluorescent Supramolecular Organic Frameworks Constructed by Amidinium-Carboxylate Salt Bridges. Chem. Eur. J. *27*, 15006–15012. https://doi.org/10.1002/chem.202102296.
61. Williams, N.J., Seipp, C.A., Brethomé, F.M., Ma, Y.-Z., Ivanov, A.S., Bryantsev, V.S., Kidder, M.K., Martin, H.J., Holguin, E., Garrabrant, K.A., and Custelcean, R. (2019). CO2 Capture via Crystalline Hydrogen-Bonded Bicarbonate Dimers. Chem *5*, 719–730. https://doi.org/10.1016/j.chempr.2018.12.025.
62. Manganaro, N., Pisagatti, I., Notti, A., Pappalardo, A., Patanè, S., Micali, N., Villari, V., Parisi, M.F., and Gattuso, G. (2018). Ring/Chain Morphology Control in Overall-Neutral, Internally Ion-Paired Supramolecular Polymers. Chem. Eur. J. *24*, 1097–1103. https://doi.org/10.1002/chem.201703342.
63. Notti, A., Pisagatti, I., Nastasi, F., Patanè, S., Parisi, M.F., and Gattuso, G. (2021). Stimuli-Responsive Internally Ion-Paired Supramolecular Polymer Based on a Bis-pillar[5]arene Dicarboxylic Acid Monomer. J. Org. Chem. *86*, 1676–1684. https://doi.org/10.1021/acs.joc.0c02501.
64. Fatila, E.M., Twum, E.B., SenGupta, A., Pink, M., Karty, J.A., Raghavachari, K., and Flood, A.H. (2016). Anions stabilize each other inside macrocyclic hosts. Angew. Chem. Int. Ed. Engl. *55*, 14057–14062. https://doi.org/10.1002/anie.201608118.
65. Zhao, W., Qiao, B., Chen, C.H., and Flood, A.H. (2017). High-Fidelity Multistate Switching with Anion-Anion and Acid-Anion Dimers of Organophosphates in Cyanostar Complexes. Angew. Chem. Int. Ed. Engl. *56*, 13083–13087. https://doi.org/10.1002/anie.201707869.
66. Mata, I., Alkorta, I., Molins, E., and Espinosa, E. (2012). Electrostatics at the origin of the stability of phosphate-phosphate complexes locked by hydrogen bonds. ChemPhysChem *13*, 1421–1424. https://doi.org/10.1002/cphc.201200068.
67. Weinhold, F., and Klein, R.A. (2014). Anti-electrostatic hydrogen bonds. Angew. Chem. Int. Ed. Engl. *53*, 11214–11217. https://doi.org/10.1002/anie.201405812.
68. Fatila, E.M., Pink, M., Twum, E.B., Karty, J.A., and Flood, A.H. (2018). Phosphate-phosphate oligomerization drives higher order co-assemblies with stacks of cyanostar macrocycles. Chem. Sci. *9*, 2863–2872. https://doi.org/10.1039/c7sc05290a.
69. Azofra, L.M., Elguero, J., and Alkorta, I. (2020). Stabilisation of dianion dimers trapped inside cyanostar macrocycles. Phys. Chem. Chem. Phys. *22*, 11348–11353. https://doi.org/10.1039/d0cp01321h.
70. Zhao, W., Flood, A.H., and White, N.G. (2020). Recognition and applications of anion-anion dimers based on anti-electrostatic hydrogen bonds (AEHBs). Chem. Soc. Rev. *49*, 7893–7906. https://doi.org/10.1039/d0cs00486c.
71. Belieres, J.-P., and Angell, C.A. (2007). Protic ionic liquids: preparation, characterization, and proton free energy level representation. J. Phys. Chem. B *111*, 4926–4937. https://doi.org/10.1021/jp067589u.
72. Stoimenovski, J., Izgorodina, E.I., and MacFarlane, D.R. (2010). Ionicity and proton transfer in protic ionic liquids. Phys. Chem. Chem. Phys. *12*, 10341–10347. https://doi.org/10.1039/c0cp00239a.
73. Amarasekara, A.S. (2016). Acidic ionic liquids. Chem. Rev. *116*, 6133–6183. https://doi.org/10.1021/acs.chemrev.5b00763.
74. Haskins, M.M., Lusi, M., and Zaworotko, M.J. (2022). Supramolecular Synthon Promiscuity in Phosphoric Acid-Dihydrogen Phosphate Ionic Cocrystals. Cryst. Growth Des. *22*, 3333–3342. https://doi.org/10.1021/acs.cgd.2c00150.
75. Aboudzadeh, M.A., Muñoz, M.E., Santamaría, A., Fernández-Berridi, M.J., Irusta, L., and Mecerreyes, D. (2012). Synthesis and Rheological Behavior of Supramolecular Ionic Networks Based on Citric Acid and Aliphatic Diamines. Macromolecules *45*, 7599–7606. https://doi.org/10.1021/ma300966m.
76. Lutovsky, G.A., Gockel, S.N., Bundesmann, M.W., Bagley, S.W., and Yoon, T.P. (2023). Iron-mediated modular decarboxylative cross-nucleophile coupling. Chem *9*, 1610–1621. https://doi.org/10.1016/j.chempr.2023.04.008.
77. McGrath, N.A., Brichacek, M., and Njardarson, J.T. (2010). A Graphical Journey of Innovative Organic Architectures That Have Improved Our Lives. J. Chem. Educ. *87*, 1348–1349. https://doi.org/10.1021/ed1003806.
78. Li, J., Huang, C.-Y., Han, J.-T., and Li, C.-J. (2021). Development of a Quinolinium/Cobaloxime Dual Photocatalytic System for Oxidative C–C Cross-Couplings via H2 Release. ACS Catal. *11*, 14148–14158. https://doi.org/10.1021/acscatal.1c04073.
79. Zhao, W., Tropp, J., Qiao, B., Pink, M., Azoulay, J.D., and Flood, A.H. (2020). Tunable Adhesion from Stoichiometry-Controlled and Sequence-Defined Supramolecular Polymers Emerges Hierarchically from Cyanostar-Stabilized Anion-Anion Linkages. J. Am. Chem. Soc. *142*, 2579–2591. https://doi.org/10.1021/jacs.9b12645.

80. We found that the presence of a little water in acetonitrile lead to formation of the 2:2 species with the tertiary ammonium cation dissociated. Freshly opened bottles of acetonitrile were used in our screening studies.

81. McNally, J.S., Noll, B., Orme, C.J., and Wilson, A.D. (2015). Density functional theory analysis of the impact of steric interaction on the function of switchable polarity solvents. J. Phys. Chem. B *119*, 6766–6775. https://doi.org/10.1021/acs.jpcb.5b03167.

82. McNally, J.S., Wang, X.P., Hoffmann, C., and Wilson, A.D. (2017). Self-assembly of molecular ions via like-charge ion interactions and through-space defined organic domains. Chem. Commun. (Camb) *53*, 10934–10937. https://doi.org/10.1039/c7cc06401b.

83. Williams, S.R., Borgerding, E.M., Layman, J.M., Wang, W., Winey, K.I., and Long, T.E. (2008). Synthesis and characterization of well-defined 12, 12-ammonium ionenes: Evaluating mechanical properties as a function of molecular weight. Macromolecules *41*, 5216–5222. https://doi.org/10.1021/ma8006152.

84. Ke, C., Yang, C., Mori, T., Wada, T., Liu, Y., and Inoue, Y. (2009). Catalytic enantiodifferentiating photocyclodimerization of 2-anthracenecarboxylic acid mediated by a non-sensitizing chiral metallosupramolecular host. Angew. Chem. Int. Ed. Engl. *48*, 6675–6677. https://doi.org/10.1002/anie.200902911.

85. Li, Y., Wang, Y., Huang, G., Ma, X., Zhou, K., and Gao, J. (2014). Chaotropic-anion-induced supramolecular self-assembly of ionic polymeric micelles. Angew. Chem. Int. Ed. Engl. *53*, 8074–8078. https://doi.org/10.1002/anie.201402525.

86. Palao, E., de la Moya, S., Agarrabeitia, A.R., Esnal, I., Bañuelos, J., López-Arbeloa, I., and Ortiz, M.J. (2014). Selective lateral lithiation of methyl BODIPYs: synthesis, photophysics, and electrochemistry of new meso derivatives. Org. Lett. *16*, 4364–4367. https://doi.org/10.1021/ol501945v.

87. Zhu, H., Fan, J., Mu, H., Zhu, T., Zhang, Z., Du, J., and Peng, X. (2016). d-PET-controlled "off-on" Polarity-sensitive Probes for Reporting Local Hydrophilicity within Lysosomes. Sci. Rep. *6*, 35627. https://doi.org/10.1038/srep35627.

88. Fa, S., Shi, T.H., Akama, S., Adachi, K., Wada, K., Tanaka, S., Oyama, N., Kato, K., Ohtani, S., Nagata, Y., et al. (2022). Real-time chirality transfer monitoring from statistically random to discrete homochiral nanotubes. Nat. Commun. *13*, 7378. https://doi.org/10.1038/s41467-022-34827-z.

89. Deng, Y., Frezel, A., Mehner, F., Friedel, P., and Gaitzsch, J. (2023). Amine-bearing cyclic ketene acetals for pH-responsive and degradable polyesters through radical ring-opening polymerisation. Polym. Chem. *14*, 4275–4281. https://doi.org/10.1039/d3py00929g.

90. Denmark, S.E., Gould, N.D., and Wolf, L.M. (2011). A Systematic Investigation of Quaternary Ammonium Ions as Asymmetric Phase-Transfer Catalysts. Synthesis of Catalyst Libraries and Evaluation of Catalyst Activity. J. Org. Chem. *76*, 4260–4336. https://doi.org/10.1021/jo2005445.

91. Despite modest differences in relative populations, reaction free energies are large after accounting for the stoichiometry of the formation reaction (Figure S239).